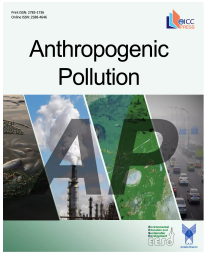

Volume 8, Issue 1, 082403 (1-10)

Anthropogenic Pollution (AP)

https://dx.doi.org/10.57647/j.jap.2024.0801.03

Land degradation intensity mapping using environmental factors and Sentinel-2 derived spectral indices in an arid region in south of Iran

Mohamamd Ebrahim Afifi[1], Raoof Mostafazadeh[2*]

[1]*Department of Geography, Islamic Azad University, Larestan Branch, Larestan, Iran.*
[2]*Department of Natural Resources, University of Mohaghegh Ardabili, Ardabil, Iran.*

[*]**Corresponding author:** raoofmostafazadeh@uma.ac.ir

Original Research

Received:
3 January 2024
Revised:
22 March 2024
Accepted:
3 April 2024
Published online:
25 June 2024

Abstract:

To mitigate land degradation and desertification as an environmntal issue, it is crucial to monitor land degradation intensities, identify influential factors, and implement necessary measures. This study utilized remote sensing data and logistic regression modeling to assess desertification in Larestan County. Multiple indicators were considered in this study, encompassing climate factors (such as rainfall, evapotranspiration, and aridity index), groundwater indicators (including electrical conductivity, chloride content, sodium absorption ratio, and groundwater level decline), soil indicators (such as EC, texture, and organic matter content), land use and land cover (LULC) type, and wind erosion. The logistic regression model was employed to identify the most influential factors contributing to desertification. The findings revealed different risk classes: a small low-risk class in the eastern and southern regions covering 2.4% of the total area, a moderate-risk class in the foothill-plain areas covering 38.3% of the total area. The high-risk class of desertification is mainly concentrated in the central part of the study area, adjacent to regions with moderate risk. It is characterized by relatively large patches, particularly in the southwest of the interior plains, covering approximately 1,980 hectares, which accounts for 7.9% of the total area. The concentration of high-risk desertification in specific areas highlights the urgent need for proactive measures to preserve the environmental balance and sustainability of the study area.

Keywords: Desertification; Land use change; NDVI; Anthropogentic degradation; Sentinel images; Logistic regression

1. Introduction

Land degradation and desertification stands out as the most significant environmental threats to dry and semi-arid regions, posing risks to human well-being and the degradation of natural resources. Thus, assessing this phenomenon holds utmost importance (Shihab and Al-hameedawi, 2020; Yousef and Jaber, 2023). The consequences of land degradation and desertification encompass reduced land fertility, expansion of abandoned areas, the emergence of dust hotspots, and the eventual rendering of the affected environemnt and their neighboring areas uninhabitable, leading to forced migration. This persistent issue extends its impact globally, affecting numerous countries, including developing nations such as Iran, and involves processes influenced by both environmental factors and human-induced improper practices(Ladisa et al., 2012; UNCCD, 2014). Desertification poses a global environmental challenge that extends beyond Iran, affecting countries worldwide, including those with more favorable and humid climates. However, the severity of this problem is particularly pronounced in Iran, where considerable amount of areas is characterized as arid to semi-arid, subject to extremely dry climatic conditions (Rahimi et al., 2014). Land use change poses a significant contemporary challenge to the environment and natural resources (Talebi Khiavi et al., 2022). Often, the initial impacts of human activities and land degradation result from positive feedback loops between biological and

non-biological processes, exacerbating degradation and impeding the system's ability to restore itself (Zolfaghari et al., 2019). Land degradation and desertification refers to the disturbance of the equilibrium among soil, vegetation cover, air, and water in dry, semi-arid, and semi-humid regions. Consequences of desertification include soil vulnerability to water and wind erosion, depletion and retreat of wetland aquifers, salinization of irrigated lands, disruption of natural vegetation regeneration, chemical degradation of the soil, and environmental consequences (Talebi Khiavi et al., 2020). Remote sensing technology plays a pivotal role in assessing and monitoring land use change, lnad degradation across local, regional, and global scales, facilitating a novel approach to studying and monitoring these phenomena (Talebi Khiavi et al., 2022).

Pan and Li (2013)) used Landsat 7 TM satellite images to extract a desertification risk map in western China. In their research, they used the technique of analyzing the spectral index pair of albedo and vegetation cover to extract a desertification intensity map. The results indicated an acceptable efficiency of 93 percent and features such as simplicity, easy access, and high accuracy in desertification mapping. Becerril-Pina et al. (2015) employed Landsat 7 TM satellite images and various indices, including NDVI, bare soil index, and albedo. Utilizing the vector analysis method, they investigated the desertification trend from 1993 to 2011 in the central part of the Mexican plateau. The study resulted in a desertification degree map and the calculation of different classes of desertification expansion in the region. Ge et al. (2016) found that changing land use intensity significantly impacted long-term bare sand land extent in Horqin Sandy Land, China. Short-term effects were linked to auto-correlation and annual precipitation, while sand dune improvement was recognized as a measure to reduce desertification risk. Lamchin et al. (2016) conducted a study in the Hogno Khaan protected area in Mongolia, aiming to develop a quantitative method for assessing land cover change and desertification using Landsat TM/ETM+ data. They utilized NDVI, TGSI, and land surface albedo as indicators of land surface conditions and found an increasing trend in desertification, with a significant increase in non-desertification and severe desertification areas from 2002 to 2011. Karimi and Namdari (2019) evaluated the intensity of desertification occurrence in Iran using Landsat satellite images and spectral mixture analysis techniques. Shihab and Al-hameedawi (2020) employed a multi-criteria evaluation method, incorporating the analytical hierarchy process and GIS, to assess desertification hazard zonation in central Iraq. Factors like aspect, slope, rainfall, temperature, land use, and wind speed were considered. In the Middle Moulouya Basin, Morocco, Lamaamri et al. (2023) utilized Sentinel-2 images and spectral index techniques to map desertification in 2018, revealing 86.86% of the area experiencing moderate to extreme desertification. Yousef and Jaber (2023) utilized remote sensing and GIS to study Bahr Al-Najaf, Iraq, finding severe desertification from 2015 to 2021, particularly in the western parts, characterized by wind erosion, dunes, and water scarcity. Studies conducted by Azzouzi et al. (2018), Farah et al. (2021), Nzuza et al. (2021), and Kumar et al. (2022) have utilized Sentinel-2 imagery and environmental factors to evaluate land degradation and desertification.

A variety of methodologies is applied for land degradation assessment, encompassing spatial analysis using Geographic Information System (GIS) and Remote Sensing (RS), as well as ground-based assessments involving field surveys, soil quality measurements, and vegetation cover assessments. The process involves monitoring Land Use and Land Cover (LULC) changes and integrating socio-economic indicators to predict land degradation. This predictive modeling utilizes statistical models and data mining techniques within multidisciplinary frameworks.

The literature review highlights the effective utilization of remote sensing techniques and spectral indices for assessing and mapping desertification across diverse regions. Landsat and Sentinel-2 satellite images, recognized for their accessibility and capability to capture multi-temporal data, have been extensively employed in these studies. There is still a research gap in understanding key factors influencing desertification and land degradation assessment. Further investigations are needed to comprehend the relative importance of climate, land use, and vegetation cover across regions. Comparative studies in different geographic locations are essential for analyzing desertification patterns, providing insights into similarities, differences, and region-specific strategies for mitigation and adaptation. Future research should prioritize developing practical models to enhance our understanding of desertification processes and inform effective management strategies. The objective of this study was to evaluate desertification in Lar County through the utilization of remote sensing data and logistic regression modeling. The assessment aimed to determine the extent of degradation by considering multiple indicators associated with regional conditions, including climate factors, groundwater indicators, soil indicators, vegetation cover percentage, land use type, and wind erosion. By employing the logistic regression model, the study identified the key factors influencing desertification and classified different areas into low-risk, moderate-risk, and high-risk zones based on the observed severity of desertification.

2. Materials and Methods

2.1 Geographical setting of the study area

The Larestan county spans an area of approximately 12,311 km^2, representing approximately 10% of Fars Province's total area (Figure 1). Larestan shares borders with Darab and Zarrindasht counties to the north, Joim, Ooz, Grash, and Lamard counties to the west, and Hormozgan Province to the east and south. In terms of administrative divisions Larestan county comprised 5 districts, 8 cities, and 11 rural districts, which ranks among the largest counties in Fars Province in terms of area, with an average elevation of 550 m above sea level. Larestan is considered arid and warm, characterized by moderate winters and extremely dry summers. The region's average annual temperature is

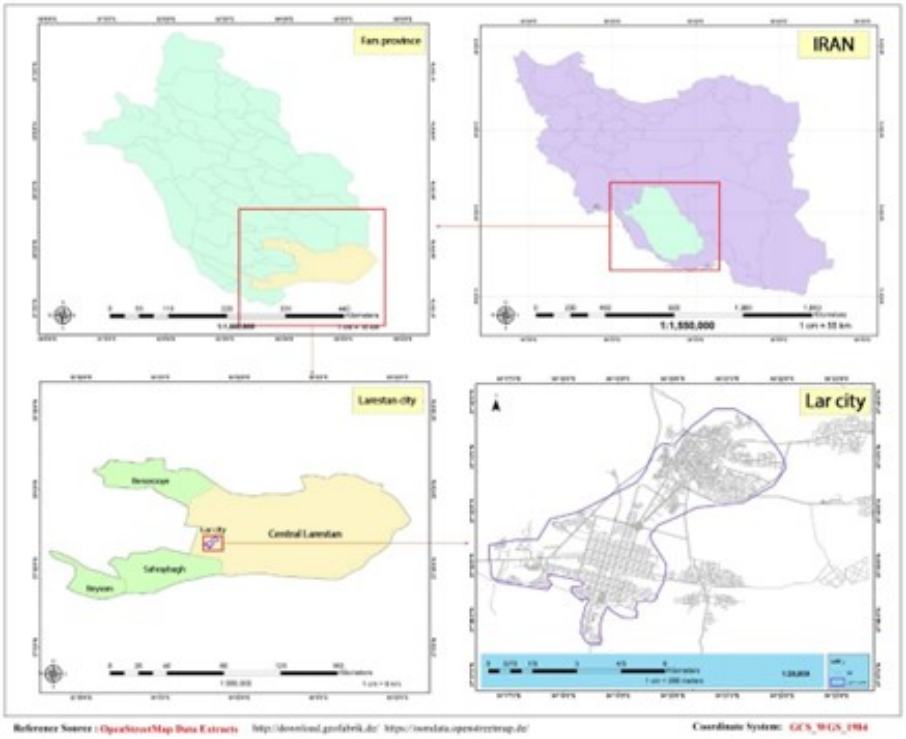

Figure 1. The geographical location of the study area.

38 degrees Celsius, with an annual average precipitation of 203 mm. The highest annual rainfall occurs in the months of December and January, featuring low intensity and prolonged duration. In contrast, precipitation reaches its minimum in July and August. The limited rainfall and arid conditions have led to poor vegetation cover in this area.

2.2 Methodology

2.2.1 Data analysis

In line with the research objectives, data and information were initially gathered for identifying influential factors contributing to desertification in specific regions. Spatial modeling using an appropriate regional model (Hu et al., 2020) was conducted. Sentinel-2 Landsat series (Level-1C) were employed to create a desertification intensity map for the study area in 2010, 2015, and 2020. These images were processed and sliced using SARscape software, aligning them with the study area boundaries (Lamaamri et al., 2023). The acquired data established a spatial baseline and generated an interferogram. Analyzing the relationships between spectral indices and desertification intensity led to determining the optimal combination of spectral indices (and Debeir, 2023). Subsequently, spectral indices were processed, and correlation analysis identified various degrees of desertification intensity (Yue et al., 2010).

Following the identification of criteria and influential indices for the desertification phenomenon, the selection process was guided by regional conditions, available data, and a comprehensive review of relevant resources in line with research objectives (Alherbawi et al., 2022). The chosen indices included climate factors (precipitation, evapotranspiration, and aridity index), groundwater criteria (electrical conductivity, chloride content, sodium absorption ratio, and static water level decline), soil criteria (electrical conductivity, texture, and organic matter content), percentage of vegetation cover, and land use types.

2.2.2 Modeling the areas susceptible to desertification

Informational layers were imported into IDRISI software for a logistic regression analysis assessing desertification susceptibility (Djeddaoui et al., 2017). The logistic regression model used zones with severe and moderately severe risk as dependent variables (Mihi et al., 2022). The key factors contributing to desertification were modeled, with these factors serving as independent variables in the logistic regression model. This comprehensive evaluation resulted in a classified map depicting desertification levels. TerrSet and ArcGIS software were utilized for data analysis, processing, modeling, and land use classification.

2.2.3 Accuracy assessment of the spatial desertification modelling

The receiver operating characteristic (ROC) curve is a widely used and effective quantitative method for evaluating model accuracy (Xu et al., 2015; Abdel-Kader, 2019). It is particularly valuable for discerning properties and probabilistically identifying and predicting systems. The area under the ROC curve indicates the model's capability to accurately estimate the occurrence or non-occurrence of desertification phenomenon. Interpretation of the Area Under the Curve (AUC) based on a rough classifying system is as follows: AUC values of 90-100 are considered excellent, 80-90 are considered good, 70-80 are considered

resonable, 60-70 are considered poor, and 50-60 are considered very poor (Safari et al., 2016).

3. Results and Discussion

3.1 Analysis of influencing factors on desertification

3.1.1 Spatial variation of groundwater condition

Regarding the assessment of groundwater status, variables including electrical conductivity, chloride content, sodium absorption ratio, and water level decline were assessed. It is worth noting that the reduction in the groundwater table is considered as an indicator of groundwater depletion, influenced by excessive exploitation or a decrease in aquifer recharge. The spatial variations of the groundwater criterion during the studied periods are illustrated in Figure 2.

3.1.2 Spatial-temporal variation of climatic cariables

The analysis of climate variable trends plays a crucial role in understanding the influence of climate on water-related systems. To assess the significance of temporal changes in precipitation, evaporation, and aridity index, the Mann-Kendall test and Sen's slope estimator were utilized in this study. The annual trend analysis results for these climate variables at the synoptic stations surrounding the study area are presented in Table 1.

The analysis of climate change conditions in the region, considering the trends in precipitation, evapotranspiration, and drought index from 2010 to 2020, reveals a predominant decreasing trend in precipitation at most stations. However, no statistically significant changes were detected ($p<0.05$). On the other hand, both evapotranspiration and drought index variables exhibited an increasing trend over the study period, with statistically significant trends observed at most stations ($p<0.05$). The map illustrating the climate criterion status is presented in Figure 3.

The intensity of desertification, as measured by this criterion, is classified as severe and very severe degradation. Specifically, due to the region's low average precipitation of around 200 mm, over 90% of the area is categorized as severely or very severely degraded. Regarding the

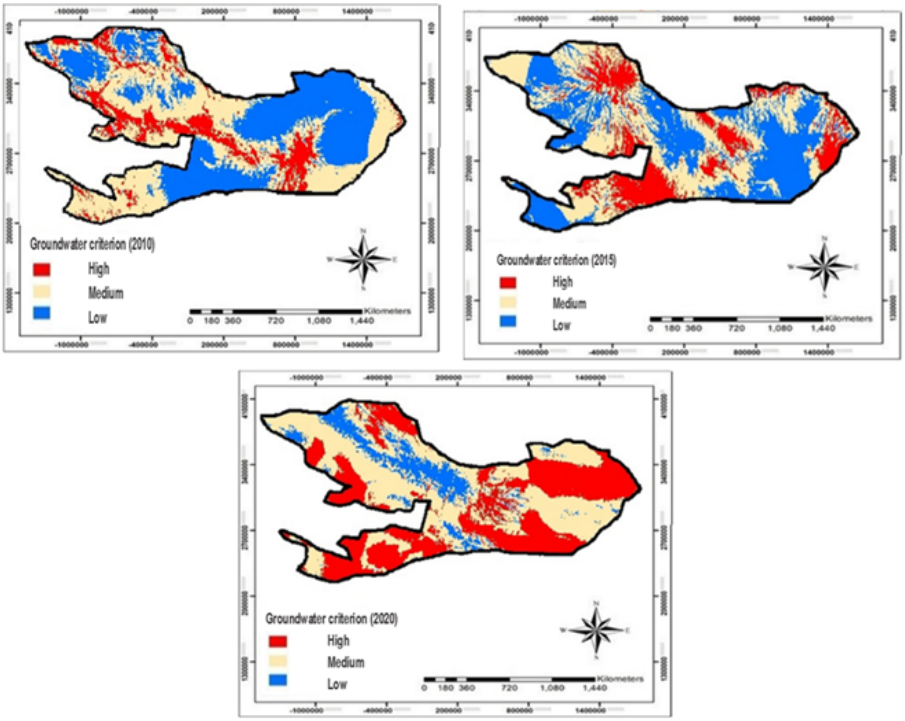

Figure 2. Spatial variations of the groundwater criterion during the studied periods.

Table 1. The results of the Mann-Kendall trend analysis test for the variables of precipitation, aridity, and evapotranspiration in the study area during the years 2010 to 2020.

Station	Precipitation		Evaporation		Aridity index	
	p-value	Sen's slope	p-value	Sen's slope	p-value	Sen's slope
Bariz	0.398	-1.317	0.095	1.914	1.093	0.073
Bayram	0.990	-0.072	0.951	0.561	0.591	0.021
Joiam	0.372	0.146	0.0030	3.591	0.0003	0.075
Fishour	0.285	-1.043	0.0010	1.562	0.0001	0.031
Didban	0.838	-1.034	0.0010	2.949	0.0001	0.043
Lar	0.595	1.079	0.0020	-3.753	0.002	-0.064

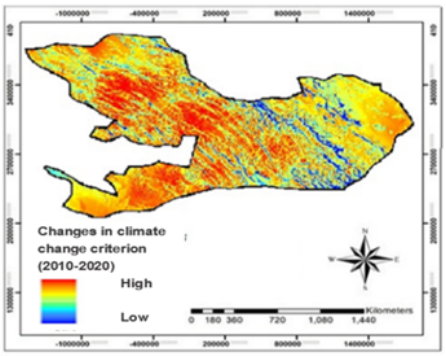

Figure 3. The variations in climatic components in the study area during the years 2010 to 2020.

climate-related indices, the evaporation index has the most significant influence, followed by the drought index and precipitation amount, in terms of degradation and desertification. These factors have particularly notable effects in the southern and western parts of the region.

3.1.3 Spatial variation of soil factor

The measured physical and chemical properties of the soil in various desertification classes are presented in Table 2 and Figure 4.

Based on the findings presented in Figure 4, notable disparities in electrical conductivity were observed in the southern and western regions of the study area, primarily due to relatively higher groundwater levels. Specifically, the electrical conductivity in these areas reached 126 decisiemens, contributing to their classification as severely desertified. Within the study area, characterized by severe and very severe desertification classes, the organic matter content exhibited substantial variations ranging from 0.61% to 5.27%. Moreover, significant discrepancies were observed in electrical conductivity and organic matter between areas with higher vegetation cover and other regions. The elevated water table in these areas, along with

Table 2. The measured soil properties that significantly contribute to the intensity of desertificatin.

Variable	Severe desertification	Very severe desertification	p-value
EC	6.4±6.2	15.5±39.8	0.000
Soil texture	33.3±2.9	30.4±6.4	0.05
Orgaic matter	5.31±0.6	1±0.7	0.05

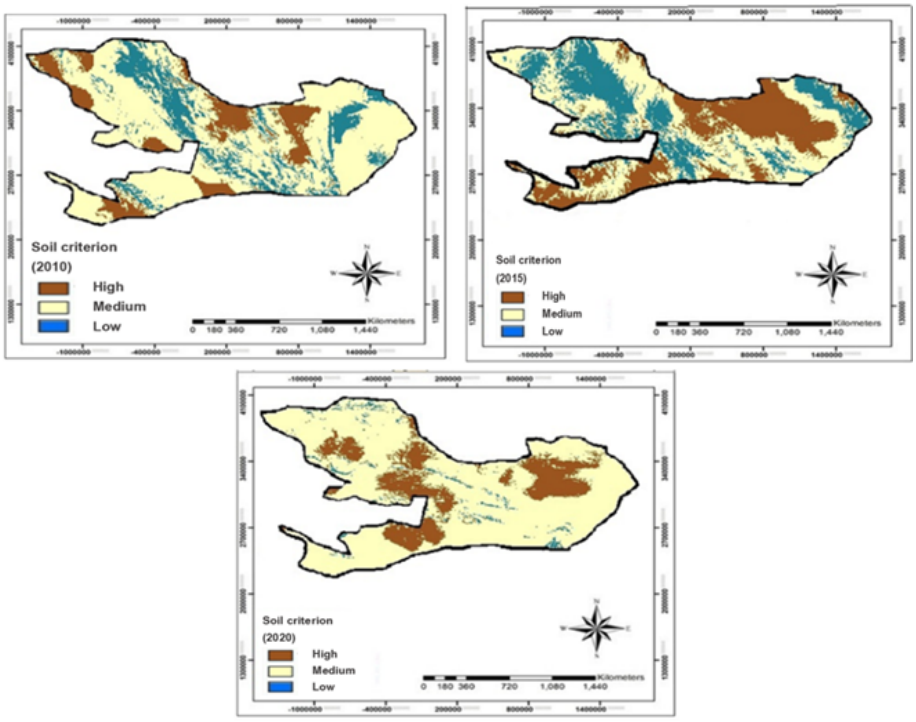

Figure 4. The impact of the soil criterion on the intensity of desertification in the study area during the study years.

the retention of salt after evaporation, accounted for the increased electrical conductivity.

The study area demonstrated a wide range of fluctuations in organic matter content. These variations can be attributed to the presence of dense cover crops, which have exerted a prolonged influence on the surface soil. The augmentation of vegetation cover has consequently led to an increase in soil organic matter content.

3.1.4 Spatial variation of vegetation cover

In this study, the TM sensor data from Landsat satellite imagery was employed to extract the vegetation cover factor and assess its spatial changes over the study years. The NDVI index values were extracted for each year, following the methodology described by Lamaamri et al. (2023) , and the obtained results are visualized in Figure 5.

The findings reveal that a significant portion of the study area, particularly the southern, western, and central regions, exhibits low NDVI values. These areas are primarily dedicated to rainfed agriculture. Field assessments conducted in the rangeland areas further indicate severe overgrazing, degradation of rangelands, conversion of such areas into agricultural lands, unsustainable utilization of rangeland byproducts, and inadequate enforcement of conservation regulations for natural resources. Consequently, the vegetation cover in these aforementioned areas has undergone significant degradation or is sparsely distributed.

3.1.5 Spatial variation of LULC

Table 3 presents the temporal changes in land use and land cover (LULC) area within the study area from 2010 to 2020. Additionally, the land use map of the study area are represented in Figures 6.

Based on the findings presented in Figure 6, there has been an increase in the Barren and Salt Marsh Lands over the 10-year period. The analysis of the provided maps reveals that the most significant decline in vegetation cover has been observed in the eastern and southern regions of Larestan County, indicating a depletion of ecological capacity in these areas. Moreover, the expansion of Barren and Salt Marsh Lands throughout the study years has resulted in the replacement of vegetation cover, leading to a reduction in ecological and biological potential and exacerbating land degradation and desertification processes.

3.1.6 Spatial overlay of effective factors on desertification

Following the calculation of the geometric mean for the assessed criteria, an overlay technique was employed to

Table 3. Changes in LULC area (km^2) of the study area during the time period from 2010 to 2020.

Year Class	2010	2015	2020
Barren/Saltmarsh	1088	1535	1672
Vegetation	1273	808	481
Built-up lands	419	450	399

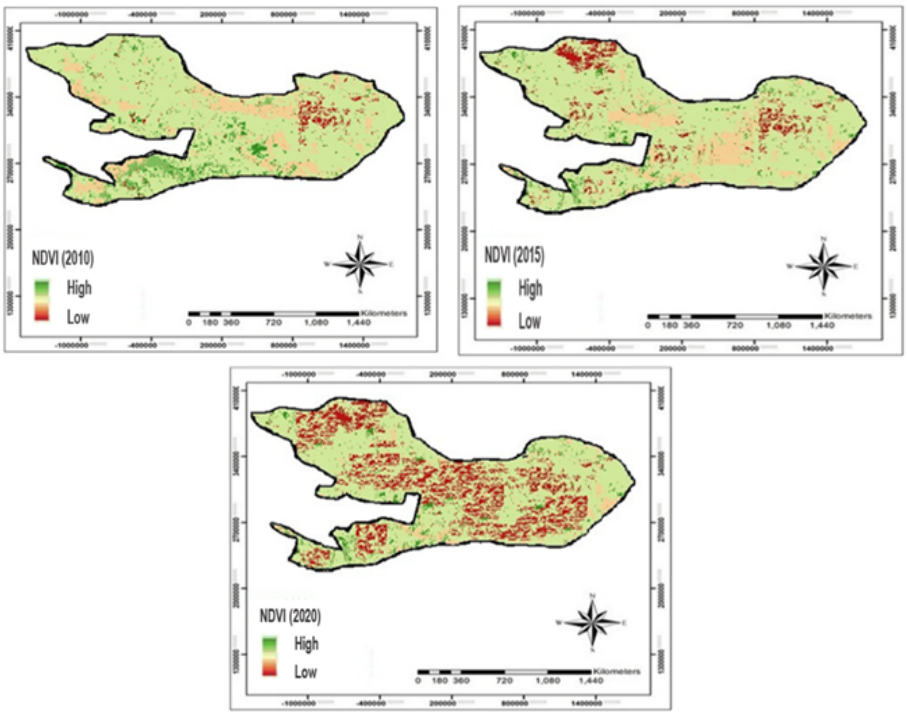

Figure 5. The map of the NDVI values across the study area throughout the examined years.

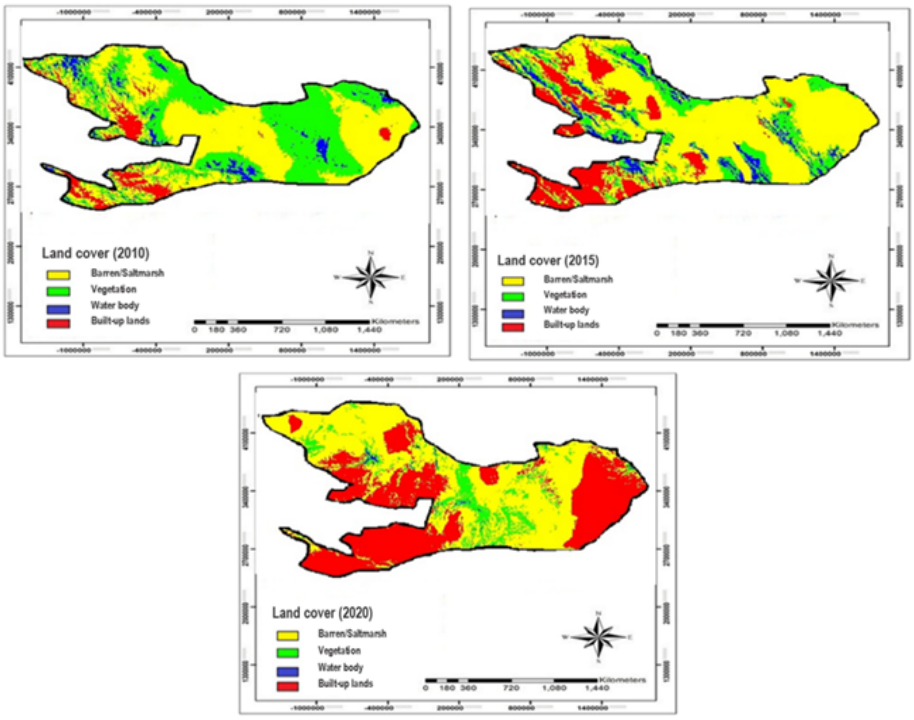

Figure 6. LULC map of the study area for the examined years.

generate the map illustrating the degradation status of the study area (Figure 7).

Based on the provided map (Figure 7), the extent of desertification intensity is as follows: 5% of the area is classified as having low desertification, 65% of the area exhibits medium desertification, and 30% of the area is categorized as severe desertification. The map reveals that the southern and eastern regions, comprising agricultural lands and rangelands, are particularly affected by severe desertification. The primary drivers of this degradation include changes in climate, vegetation cover, and land use patterns, resulting from agricultural expansion, intensified water resource utilization, and declining precipitation. Consequently, these factors have significantly contributed to the deterioration of the region. The rangelands in this specific area are classified as poor rangelands, exacerbating soil quality degradation and vegetation cover loss.

3.1.7 The desertification map derived from the logistic regression model

Following the preparation and conversion of the independent variable layers into binary values (0 and 1), the calculated coefficients for each class were utilized to generate the desertification zoning map of the region.

$$\begin{aligned}\text{Land subsidence} = {} & 0.0023 \times \text{Aspect} + 0.0012 \times \text{Dem} \\ & + 0.0003 \times \text{DistWell} + 0.948 \times \text{Luse} \\ & + 0.00026 \times \text{Lithology} + 2.622 \times \text{River} \\ & + 0.0032 \times \text{Road} - 0.0042 \times \text{Slope} \\ & - 0.004 \times \text{Village} + 6.0042 \times \text{Water table}\end{aligned}$$

The final desertification zoning map of the study area was classified into three risk classes: low, moderate, and high. The results of this classification are presented in Figure 8. Based on the obtained results, the low-risk class is

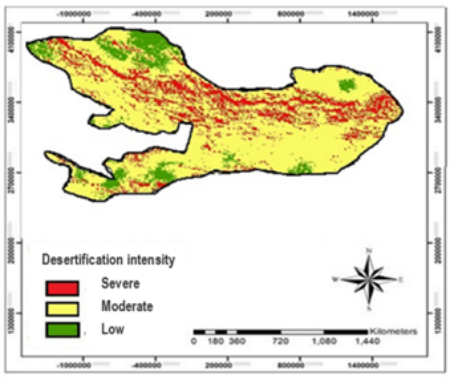

Figure 7. Map of desertification intensity based on the spatial overlay of influential factors.

predominantly observed in small sections of the eastern and southern parts of the study area, forming a narrow strip (Figure 8). This class encompasses an area of 604 hectares, representing a minor proportion of the total study area. In terms of spatial distribution, the moderate-risk class is dispersed across the foothill and plain regions, encircling the central basin of the study area in a halo-like pattern. This class covers an approximate area of 9,560 hectares, signifying a substantial portion of the total area. The high-risk class is situated in proximity to the moderate-risk areas, predominantly concentrated in the central part of the study area. It exhibits patchy characteristics within the plains of the study area and is relatively extensive in the southwestern region, encompassing an area of approximately 1,980 hectares.

3.2 Accuracy of the logistic regression model in desertification mapping

The results of accuracy and validation assessment for the logistic regression model are presented in Table 4 and Figure 9.

Based on the information presented in Table 4 and Figure 9, the logistic regression model demonstrates a strong performance with an AUC value of 0.89. This indicates a high level of accuracy in the conducted desertification risk zoning within the study area, reflecting a satisfactory level of reliability.

4. Conclusion

A regional model adhering to scientific principles is developed to identify influential factors in desertification, including climate, groundwater, soil, vegetation cover, land use type, and wind erosion. These factors are modeled using logistic regression in IDRISI software. Hazardous zones identified during desertification monitoring serve as the dependent variable, and various data, including groundwater criteria, are collected for independent variables. GIS generates spatial variation maps for the identified factors. Analysis shows an increasing trend in the study area over time, with rising groundwater salinity affecting a wide basin. Groundwater levels exhibit a decline.

Groundwater decline results from agricultural expansion, lower precipitation, and a shift to high-water-demand crops. Between 2010-2020, 2020 saw decreased precipitation, increased aridity, and evapotranspiration. With 90% falling into severe degradation categories, areas with around 200 mm rainfall are most affected. Evapotranspiration has the greatest impact on degradation, followed by aridity and precipitation indices. Higher groundwater levels in the south and west contribute to severe desertification with elevated electrical conductivity of 126 decisiemens. The region's high organic matter content is due to dense vegetation cover and long-term cultivation, leading to increased carbon and organic matter in the soil. The southern, western, and central regions, with lower vegetation cover due to drylands and agriculture, are more vulnerable to drought than rangelands. Human activities, including overgrazing, agricultural conversion, and weak resource protection laws, have led to significant vegetation loss. Over the past decade, mapping reveals a 447 sq km increase in desert and saline lands. The study classifies desertification risk into three categories: low, moderate, and high. The low-risk class appears as a narrow strip in the east and south, covering 604 hectares. The moderate-risk class is scattered in foothill and plain areas surrounding the central plain. The high-risk class is concentrated in the central

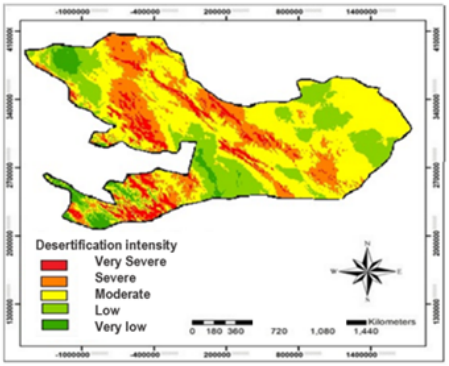

Figure 8. Desertification zoning map of the study area based on the logistic regression model.

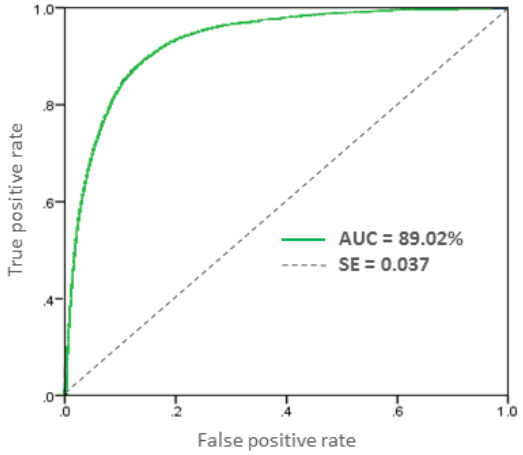

Figure 9. The ROC curve of the logistic regression model for estimating the intensity of desertification in the study area.

Table 4. The AUC, standard deviation and the corresponding confidence level.

Area	Std.Error	Asympotic Sig	Asymptopic 95% Confidence Interval	
			Upper Bound	Lower Bound
0.890	0.000	0.000	0.83	0.83

area, forming large patches in the south and southwest, particularly in the interior plains. Results depend on data quality, and spectral limits in remote sensing may bring uncertainties. The robust logistic regression model might not fully capture complex interactions due to assumptions. While comprehensive, the study may not fully address critical desertification factors, limiting understanding. Focused on Larestan County, it offers a snapshot of desertification, meanwhile, future research should detect temporal dynamics, consider projections, and integrate forces for sustainable land management strategies for enhanced understanding.

Practical desertification control in the study area should concentrate on high-risk regions, particularly in the central and southwestern areas. Implementing sustainable practices, strengthening regulations against overgrazing and unsustainable agriculture, and engaging communities in awareness programs are crucial for responsible land use and environmental management.

Authors Contributions

Authors have equal contribution role in preparing the paper.

Availability of Data and Materials

The data that support the findings of this study are available from the corresponding author upon reasonable request.

Conflict of Interests

The authors declare that they have no known competing financial interests or personal relationships that could have appeared to influence the work reported in this paper.

References

P, Debeir O (2023) Multispectral Satellite Image Analysis for Computing Vegetation Indices by R in the Khartoum Region of Sudan, Northeast Africa. *Journal of imaging* 9(5):98.

Abdel-Kader FH (2019) Assessment and monitoring of land degradation in the northwest coast region, Egypt using Earth observations data. *The Egyptian Journal of Remote Sensing and Space Science* 22(2):165–173.

Alherbawi M, McKay G, Govindan R, Haji M, Al-Ansari T (2022) A novel approach on the delineation of a multipurpose energy-greenbelt to produce biofuel and combat desertification in arid regions. *Journal of Environmental Management* 323:116223.

Azzouzi SA, Vidal-Pantaleoni A, Bentounes HA (2018) Monitoring desertification in Biskra, Algeria using Landsat 8 and Sentinel-1A images. *IEEE Access* 6:30844–30854.

Becerril-Pina R, Mastachi-Loza CA, Gonzalez-Sosa E, Dlaz-Delgado C, Ba KM (2015) Assessing desertification risk in the semi-arid highlands of central Mexico. *Journal of Arid Environments* 120:4–13.

Djeddaoui F, Chadli M, Gloaguen R (2017) Desertification susceptibility mapping using logistic regression analysis in the Djelfa area, Algeria. *Remote Sensing* 9(10):1031.

Farah A, Algouti A, Algouti A, Ifkirne M, Ezziyani A (2021) Mapping of soil degradation in semi-arid environments in the ouarzazate basin in the south of the central High Atlas, Morocco, using sentinel 2A data. *Remote Sensing Applications: Society and Environment* 23:100548.

Ge X, Dong K, Luloff AE, Wang L, Xiao J (2016) Impact of land use intensity on sandy desertification: An evidence from Horqin sandy land, China. *Ecological Indicators* 61(2):346–358. https://doi.org/10.1016/j.ecolind.2015.09.035

Hu Y, Han Y, Zhang Y (2020) Land desertification and its influencing factors in Kazakhstan. *Journal of Arid Environments* 180:10.

Karimi N, Namdari S (2019) Estimation of severity and extent of desertification in Iran using Landsat satellite images and spectral mixture analyses methods between 1984 and 2015. *Iranian Journal of Range and Desert Research* 26(2):500–515. https://doi.org/10.22092/ijrdr.2019.119369

Kumar BP, Babu KR, Anusha BN, Rajasekhar M (2022) Geo-environmental monitoring and assessment of land degradation and desertification in the semi-arid regions using Landsat 8 OLI/TIRS, LST, and NDVI approach. *Environmental Challenges* 8:100578.

Ladisa G, Todorovic M, Trisorio Liuzzi G (2012) A GIS-based approach for desertification risk assessment in Apulia region, SE Italy. *Phys. Chem. Earth. Parts A/B/C* 49:103–113.

Lamaamri M, Lghabi N, Ghazi A, El Harchaoui N, Adnan MSG, Shakiul Islam M (2023) Evaluation of desertification in the middle Moulouya basin (north-east morocco) using sentinel-2 images and spectral index techniques. *Earth Systems and Environment* 7(2):473–492.

Lamchin M, Lee J-Y, Lee W-K, Lee EJ, Kim M, Lim C-H, Choi H-A, Kim S-R (2016) Assessment of land cover change and desertification using remote sensing technology in a local region of Mongolia. *Advances in Space Research* 57(1):64–77. https://doi.org/10.1016/j.asr.2015.10.006

Mihi A, Ghazela R, Wissal D (2022) Mapping potential desertification-prone areas in North-Eastern Algeria using logistic regression model, GIS, and remote sensing techniques. *Environmental Earth Sciences* 81(15):385.

Nzuza P, Ramoelo A, Odindi J, Kahinda JM, Madonsela S (2021) Predicting land degradation using Sentinel-2 and environmental variables in the Lepellane catchment of the Greater Sekhukhune District, South Africa. *Physics and Chemistry of the Earth, Parts A/B/C* 124:102931.

Pan J, Li T (2013) Extracting desertification from Landsat TM imagery based on spectral mixture analysis and Albedo-Vegetation feature space. *Natural Hazards* 68:915–927.

Rahimi M, Damavandi AA, Jafarian V (2014) Investigating remote sensing applications in evaluating and monitoring land degradation and desertification. *Scientific-Research Quarterly of Geographical Data (SEPEHR)* 22(88):115–128.

Safari S, Baratloo A, Elfil M, Negida A (2016) Evidence Based Emergency Medicine; Part 5 Receiver Operating Curve and Area under the Curve. *Archives of Academic Emergency Medicine* 4(2):111–113. https://doi.org/10.22037/aaem.v4i2.232

Shihab TH, Al-hameedawi AN (2020) Desertification hazard zonation in Central Iraq using multi-criteria evaluation and GIS. *Journal of the Indian Society of Remote Sensing* 48:397–409. https://doi.org/10.1007/s12524-019-01054-0

Talebi Khiavi H, Mostafazadeh R, Asaadi MA, Asbaghian Namini SK (2022) Temporal land use change and its economic values under competing driving forces in a diverse land use configuration. *Arabian Journal of Geosciences* 15(20):1597.

Talebi Khiavi H, Shafizadeh Moghadam H, Karimian Eghbal M (2020) Modeling the probability of gully occurrence and investigating the spatial effects of its drivers using the boosted tree regression. *Environmental Sciences* 18(3):167–183.

UNCCD (2014) Desertification: The Invisible Frontline. *UNCCD Publications: Bonn, Germany*

Xu EQ, Zhang HQ, Li MX (2015) Object-based mapping of karst rocky desertification using a support vector machine. *Land Degradation & Development* 26(2):158–167.

Yousef OAR, Jaber HS (2023) Study of desertification in Bahr Al-Najaf region by remote sensing data and GIS. *AIP Conference Proceedings* 2775:050010. https://doi.org/10.1063/5.0159667

Yue Y, Zhang B, Wang K, Liu B, Li R, Jiao Q, Zhang M … (2010) Spectral indices for estimating ecological indicators of karst rocky desertification. *International Journal of Remote Sensing* 31(8):2115–2122.

Zolfaghari F, Khosravi H, Shahriyari A, Jabbari M, Abolhasani A (2019) Hierarchical cluster analysis to identify the homogeneous desertification management units. *PloS one* 14(12):e0226355.